Automatic Information Gain-guided Convergence for refining building design parameters: Enhancing effectiveness and interpretability in Simulation-based Optimization

Qianyun Zhou[1], Fan Xue[2]*

Abstract

Simulation-based optimization (SBO) is widely applied to building designs by iteratively tuning design parameters towards sustainable goals. However, numerous design parameters in exploratory stages lead to design uncertainty and exponentially increase optimization search space's dimensionality. The non-linear, non-derivative nature of objective functions determines SBO tasks a black box, which lacks interpretability for design decisions or optimization strategies. This study introduces an Automatic Information Gain-guided Convergence (AIGGC) method for refining critical design parameters in building performance SBO. The AIGGC method extends the generic SBO process with interpretable and interoperable information gain analysis for each design parameter and component, to converge to the most promising domain sub-intervals prior to traditional SBOs. Experimental results evaluated the robustness and scalability of AIGGC across two design scales. Under the same iteration budgets, AIGGC significantly enhanced three SBO algorithms, i.e., RBFOpt, CMAES, and GA, by 0.62~0.67% less energy use intensity and 2.14~4.74% more direct sunlight hours against the baseline solutions, respectively. The contribution of this study involves two aspects, including introducing a novel information-theory-based method for optimizing design parameters in high-dimensional SBO tasks of sustainable building designs, and a novel perspective in guiding stakeholders with interpretable analysis of building design parameters.

Keywords: Information gain; Simulation-based optimization; Sustainable building design; Interpretability analysis

[1] Qianyun Zhou, MArch,
PhD student, Department of Real Estate and Construction, The University of Hong Kong, Pokfulam, Hong Kong, China
E-mail: qianyun8@connect.hku.hk ORCiD: https://orcid.org/0000-0002-5466-6225

[2] Fan Xue, PhD
Associate Professor, Department of Real Estate and Construction, The University of Hong Kong, Pokfulam, Hong Kong, China
E-mail: xuef@hku.hk ORCiD: https://orcid.org/0000-0003-2217-3693
* Corresponding author, Tel: +852 3917 4174, Fax: +852 2559 9457, Email: xuef@hku.hk

Highlights

- A novel Information Gain-guided parameter convergence for complex sustainable designs
- A sound information-theory-based method to enhance generic simulation-based optimization (SBO)
- Automatic converging design parameters to most promising domain sub-intervals
- Improved 3 SBO algorithms in 2 cases, by 0.62~0.67% less energy cost and 2.14~4.74% more sunlight hours
- Interpretable guidance for stakeholders in sustainable design decision-making

1 Introduction

The building and construction sector significantly contributes to global climate change, accounting for 34 percent of global energy demand and 37 percent of greenhouse gas emissions (UNEP 2024). Nowadays, the sector follows sustainable planning guidelines and standards among countries, focusing on reducing building energy consumption and enhancing occupant well-being to create environmentally friendly buildings and urban neighborhoods (Luca et al. 2024; He et al. 2024). The environmental performance analysis of buildings includes various aspects, such as energy consumption, thermal comfort, and daylighting (Zhan et al. 2024). Extensive research has shown that early-stage building design is critical to effectively enhancing these performance outcomes (Wang et al. 2024). By integrating simulation engines into visual programming environments, parametric modeling techniques can couple with simulation data to deliver instant performance feedback during design generation (Hinkle et al. 2024).

Simulation-based optimization (SBO) automates the design exploration process through iterative algorithms, enabling the identification of optimal or near-optimal solutions with less time and labor (Nguyen et al. 2014). Typically, an SBO process begins with defining the target design parameters and objective function, followed by an optimizer iteratively updating the design parameters to converge towards the optimal solution. Early-stage building design often involves a vast range of parameters that control the building's physical components, materials, and systems (Wang et al. 2024; Zhan et al. 2024; Es-sakali et al. 2025). A large number of design parameters results in the uncertainty of potential designs and the exponential growth of the design search space, known as the 'curse of dimensionality' (Nguyen et al. 2014; Chen et al. 2015; Han et al. 2023). The high dimensionality of the search space complicates SBO convergence; furthermore, time-intensive simulations plus limited iteration budgets confine the efficiency in SBO. On the other hand, the non-linear, non-derivative nature of objective functions makes SBO a black box (Waibel et al. 2019), which limits interpretability for decision-makers and provides little insight into guiding the convergence of the design search space.

Current frontier research employed sensitivity analysis techniques to quantify the importance of design parameters (Østergård et al. 2017; Brown & Mueller 2019; Hinkle et al.

2024). Some studies have incorporated surrogate models to replace simulation engines in SBO, enabling real-time interactive optimization (Lin et al. 2021; Han et al. 2023; Li et al. 2024). Others have explored visual analytics to enhance the interpretability of SBO results (Showkatbakhsh & Makki 2022). However, both sensitivity-based techniques and surrogate models rely on extensive simulation datasets for analysis and often need rerunning for different optimization tasks, requiring considerable time and labor. Additionally, while visualizing optimization results improves interpretability, it does not enhance optimization efficiency, leaving a research gap in improving the interpretability of the optimization convergence process.

The uncertainty and lack of interpretability in high-dimensional SBO search spaces make it challenging for stakeholders to fully understand the SBO process. In this context, information entropy, a classical concept in information theory (Shannon 1948), provides the fundamental measure of uncertainty within a variable or dataset. The entropy reflects the amount of information gained when observing the outcome of a potential state. Information gain (IG), that quantifies changes in information entropy, is a classic descriptor for assessing feature importance during data partitioning (Zhang et al. 2022). IG is, therefore, widely applied in many fields, such as machine learning and data mining, to address the curse of dimensionality while enhancing model interpretability and decision-making capability (Omuya et al. 2021; Son & Hyun 2022). However, in the building and construction sector, few studies have conducted IG-based methods or analyses for SBO tasks.

Our research aims to enhance the generic SBO process by incorporating IG-guided analysis for each design parameter and component, optimizing the initial parameter set to those most promising for improving building performance and thereby reducing the dimensionality of the search space. Additionally, the visualized results of IG-guided analysis provide interpretable insights for stakeholders, enabling them to independently navigate optimization convergence, and enhancing their understanding of the process.

Therefore, this paper presents an Automatic IG-guided Convergence (AIGGC) method for refining design parameters in sustainable building designs. This method allocates a small portion of the iteration budget for first-phase optimization, using its results to conduct IG-guided analysis of sub-intervals within each design parameter. This analysis aids stakeholders in automatically converging design parameters and identifying high-quality interval domains. The remaining iteration budget is then applied to re-optimize the converged parameters, further improving the solution. This paper tested the robustness and scalability of the proposed method on two prominent optimization objectives: minimizing the annual energy consumption of a typical modular flat in Hong Kong and maximizing sunlight hours on the ground floor of a south-facing urban block in Jianhu City. The contribution of this paper is thus twofold: (i) a novel information-theory-based method for optimizing design parameters in high-dimensional SBO tasks of sustainable building designs, and (ii) a novel perspective in guiding stakeholders with interpretable analysis of building design parameters.

2 Literature review

2.1 Simulation-based optimization for buildings and construction

SBO is recognized as a commonly used strategy for satisfying the sustainable requirements of high-performance building designs, both in research and practice. Since the late 2000s, the workflow of iteratively coupling optimization algorithms with simulation programs to approximate sub-optimal solutions has gained popularity (Evins 2013; Nguyen et al. 2014; Javanroodi et al. 2019). The generic SBO process can be divided in three phases: the first phase is the definition of the optimization task, including setting independent design parameters, objective functions, and constraints; then it follows by running optimization algorithms while monitoring convergence; and finally, the optimized data is transformed into visualized charts (Nguyen et al. 2014; Zhan et al. 2024).

Optimization is the process of discovering the minimum or maximum of a function by selecting certain variables under given constraints (Machairas et al. 2014; Yu et al. 2023). In SBO, the objective function is typically a "black box" computed by third-party simulation engines, relying on complex physical models and climate data, making direct mathematical formulation infeasible (Evins 2013; Cruz et al. 2024). The highly non-linear, non-derivative mapping of multi-dimensional inputs defines SBO as a black-box optimization problem (Wortmann 2019; Waibel et al. 2019). Consequently, derivative-free algorithms, including Genetic Algorithm (GA), Particle Swarm Optimization (PSO), Simulated Annealing (SA), Covariance Matrix Adaptation Evolution Strategy (CMA-ES), and RBFOpt, are widely employed in architectural design exploration (Machairas et al. 2014; Waibel et al. 2019). Statistics show that GA is the most frequently used among these algorithms (Evins 2013; Nguyen et al. 2014), while comparative studies have found that CMA-ES and RBFOpt outperform in black-box optimization for building design (Kämpf et al. 2010; Xue et al. 2019; Wortmann 2019; Rehbach et al. 2022).

Energy performance optimization has been extensively studied in SBO tasks to mitigate buildings' environmental impact (Evins 2013; Luca et al. 2024). By integrating energy simulation engines such as EnergyPlus, TRNSYS, and DOE-2, key metrics like cooling and heating loads and Energy Use Intensity (EUI) can be evaluated (Nguyen et al. 2014). Among building components, optimizing orientation, layouts, HVAC systems, envelope design, and openings play a crucial role in passively reducing energy consumption (Konis et al. 2016; Javanroodi et al. 2019; Mousavi et al. 2022; Gupta & Deb 2023; Zhou & Xue 2023). Notably, envelope optimization is essential for substantial energy savings, with studies showing reductions of up to 50% (Es-sakali et al. 2025). Optimizing the building envelope involves multiple factors, including wall materials, window-to-wall ratio (WWR), window shape, glazing, and shading (Hinkle et al. 2022; Wortmann et al. 2022). Among these, studies identify WWR as a major factor influencing building energy consumption (Wang et al. 2024).

Daylight quality is also a crucial aspect of sustainable design exploration, serving as a critical indicator of livability and well-being (Fang & Cho 2019; Bushra 2022; Luca et al. 2024).

In the built environment, daylight accessibility is influenced by inter-building overshadowing, and numerous studies have shown that optimizing block morphology and layout can significantly enhance regional daylight quality (Javanroodi et al. 2019; Liu et al. 2023; Liu et al. 2024).

Nowadays, researchers have developed a range of tools on Grasshopper and Dynamo platforms to integrate the whole generic SBO process, enabling architects to seamlessly transition from parametric modeling to simulation engines (e.g., Diva, Radiance, Honeybee, and Ladybug), and finally to optimizers and visualization tools such as Galapagos, Octopus, Wallacei, and Opossum (Javanroodi et al. 2019; Wortmann et al. 2022; Luca et al. 2024). However, given the high-dimensional design search space generated by numerous design parameters in early design stages, combined with the black-box nature of SBO, the generic SBO process still faces limitations in search efficiency and the interpretable guidance for optimization convergence.

2.2 Design parameter analysis for convergence of search space

The memory and computational cost may rise exponentially and become difficult to navigate as more design parameters are brought into the SBO task (Nguyen et al. 2014). In practice, the convergence of design parameters is heavily influenced by the designer's prior knowledge (Brown & Mueller 2019; Wang et al. 2024). However, this process can be particularly challenging for other stakeholders with little design experience. Therefore, implementing a systematic converging and analysis approach in the early design stages is essential to maintain a manageable and effective set of design parameters.

Previous studies have conducted design parameters analysis through literature reviews (Zhou et al. 2023), sensitivity analysis (Tian 2013; Østergård et al. 2017), or machine learning-based feature selection method (Olu-Ajayi et al. 2022; Liu et al. 2022; Hinkle et al. 2024). Zhou et al. (2023), for instance, reviewed 50 papers published between 2010 and 2022, summarizing eight types of design parameters that significantly impact building environmental performance. This review helps to focus on the categories of design parameters in SBO. Sensitivity analysis is commonly divided into local and global approaches (Tian 2013), with global sensitivity analysis being more widely used in building analysis due to the non-linear, multi-modal, and discontinuous character of building simulation results (Nguyen et al. 2014). Global sensitivity analysis methods include regression techniques (e.g., Standardized Regression Coefficients and Standardized Rank Regression Coefficients), screening-based methods (e.g., the Morris method), variance-based methods (e.g., Fourier Amplitude Sensitivity Test and Sobol method), and meta-modeling approaches (e.g., Multivariate Adaptive Regression Splines and Support Vector Machines). Machine learning-based feature selection methods, such as Random Forest (RF) or Extra Trees classifiers, apply recursive assessment of feature importance by evaluating the effect of adding or removing individual features (Olu-Ajayi et al. 2022; Liu et al. 2022; Tian et al. 2024).

While Zhou et al. (2023) emphasize the categories of design parameters in SBO, it has a limited impact on reducing the dimensionality of the optimization search space. In contrast, most global sensitivity analyses require extensive large-scale sampling techniques, such as Monte Carlo or Latin Hypercube Sampling, which is impractical for SBO tasks with time-intensive simulations, as each simulation can take several minutes or even hours (Tian 2013; Nguyen et al. 2014; Østergård et al. 2017). Additionally, machine learning-based feature selection methods provide important metrics through training; however, if variables or their value boundaries change, retraining becomes necessary to maintain accuracy, which increases computational costs (Hinkle et al. 2024). Therefore, effectively screening design parameters without increasing computational burden and seamlessly integrating this process into the SBO workflow remains a research challenge in SBO tasks.

2.3 Information gain and applications

Given the uncertainty and lack of interpretability in high-dimensional SBO, information theory provides a possible approach to addressing these challenges. In information theory, information entropy is proposed as the metric for uncertainty or randomness within a dataset (Shannon 1948). And information gain (IG) is an entropy-based feature evaluation method widely used in machine learning (Zhang et al. 2022). In decision trees, it helps to choose the feature that best splits the data, with higher IG indicating more effective sample separation and improved classification (Kotsiantis 2013). Chen and Hao (2017) applied IG to rank feature importance in stock market indices prediction, providing a basis for computing feature weights in weighted Support Vector Machines. Besides, Omuya et al. (2021) utilized an IG-based feature selection technique to address the curse of dimensionality, improving the accuracy and overall performance of machine learning algorithms.

In the building design sector, limited research has integrated information entropy or information gain. Hester et al. (2018) were the first to apply information entropy in early-stage building design optimization, quantifying the flexibility of uncertain or probabilistic designs during iterative refinement and optimization. Son et al. (2022) developed a proactive design exploration system incorporating Bayesian information gain and information entropy to provide designers with guidance feedback during the design exploration process. Additionally, other researchers employed information gain to determine criterion weights in multi-criteria decision-making (Weerasuriya et al. 2021; Zhang et al. 2022). However, information gain-guided methods remain scarce in high-dimensional SBO tasks, revealing a gap in the research.

3 Research methods

This paper demonstrates the effectiveness of the Automatic Information Gain-guided Convergence (AIGGC) method in early-stage building design through two sustainable design case studies. The overall workflow is illustrated in Figure 1.
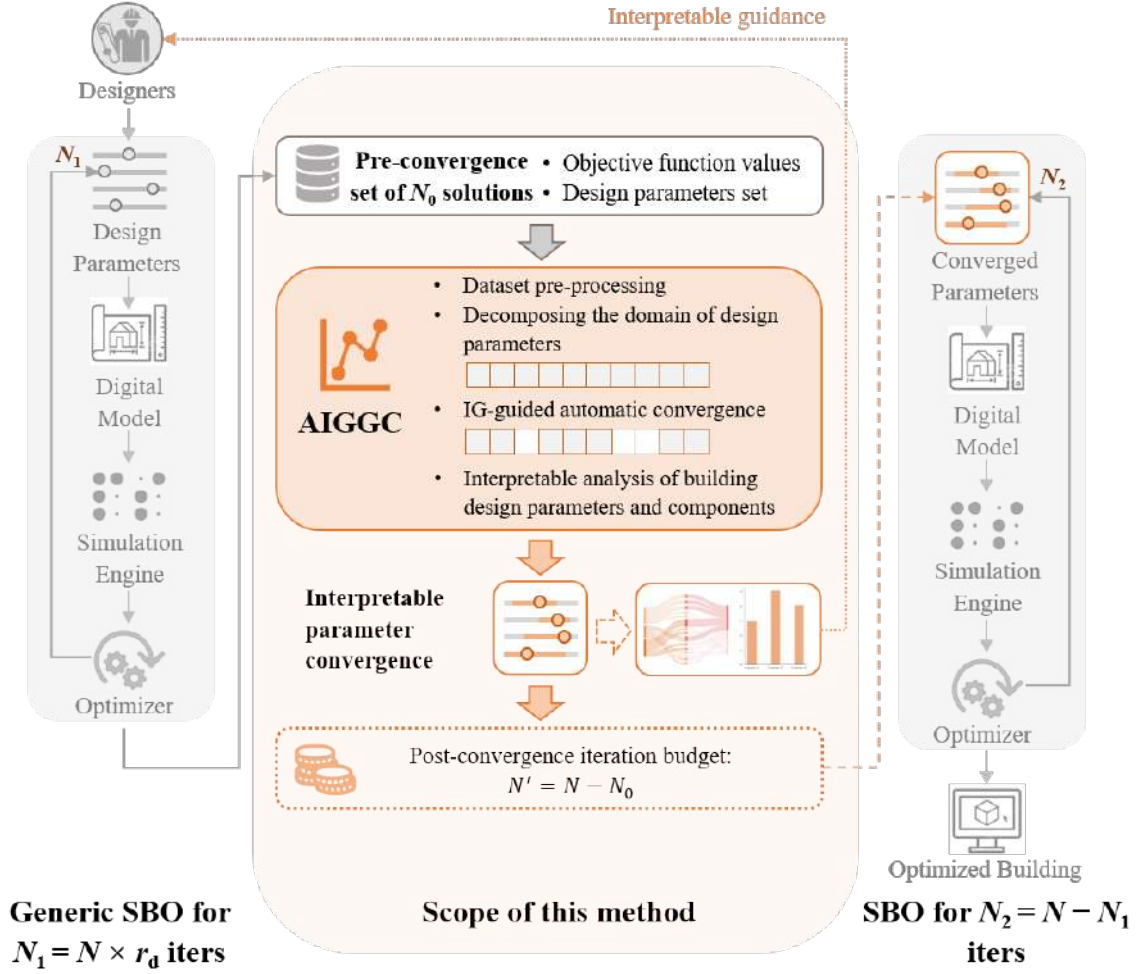
Figure 1. The proposed workflow for Automatic IG-guided Convergence of design parameters.

Distinct from the generic SBO process, which optimizes the program by running the total iteration budget once, this method allocates a small portion of the total budget for first-phase optimization. The optimized results from first-phase optimization, comprising objective function values and corresponding design parameter sets, are then utilized as a dataset for IG-guided analysis. Second, the dataset is pre-processed, and the initial domain intervals of the design parameters are partitioned. IG is then calculated for each sub-interval, enabling automatic convergence by prioritizing high-information design parameters based on the total IG score. The IG-guided visual analysis provides stakeholders with interpretable insights from both design parameters and components, allowing them to converge design parameters and gain a deeper understanding of influential components. Finally, the converged design parameters are adopted for the second phase of optimization.

3.1 Information gain-guided approach for automatic convergence

3.1.1 Design the allocation of iteration budget

As shown in Figure 1, the AIGGC method consists of two optimization phases. First, building designers set the total iteration budget (N) and determine the distribution ratio (r_d) between the

two phases, resulting in the pre-convergence budget ($N_1 = N \times r_d$) and the post-convergence budget ($N_2 = N - N_1$). In the second phase, the converged design parameters based on IG-guided visual analysis are re-inputted into the optimizer to finally find the optimal solution. The optimization settings and algorithm remain the same across both phases.

3.1.2 Dataset preprocessing

The first-phase optimization generates a dataset of optimized design solutions (S) and corresponding objective function values $f(S)$, organized as a matrix. The first row lists the names of design parameters and the objective function, while each subsequent row represents an optimized solution. The matrix is then sorted by the optimization objective in ascending order (for minimizing $f(x)$) or descending order (for maximizing $f(x)$). Subsequently, inspired by the elitism strategy in GA, the dataset is categorized into 'elite' and 'non-elite' groups based on a designer-defined elite ratio (r_e), as shown in Figure 2.
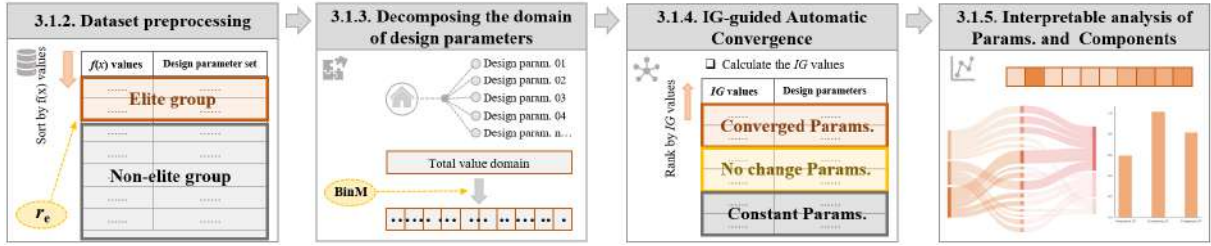

Figure 2. Detailed procedures of IG-guided automatic convergence.

3.1.3 Decomposing the domain of design parameters

The initial design parameter domains (R) are divided into multiple sub-interval bins using the partitioning method (BinM), and the number of bins (N_b) determines the analytical granularity. This partitioning process helps to analyze the distribution of pre-optimized solutions within each sub-interval bin after the first-phase optimization and to calculate the probability of solutions belonging to the 'elite' group. In addition, it aids in targeting promising regions of design parameters for further optimization.

This study proposes three approaches for the partitioning method (BinM $\in Z$): (1) BinM = 10, dividing each design parameter domain into 10 bins; (2) BinM = $N_1/10$, with the number of bins set to the integer value of the pre-convergence budget (N_1) divided by 10; (3) BinM = $\sqrt{N_1}$, with the number of bins set to the integer value of the square root of the pre-convergence budget (N_1).

3.1.4 IG-guided Automatic Convergence

The information gain (γ) for each design parameter can be computed automatically according to Algorithm 1. The algorithm takes as input a set of solutions (S) with their objective function values $f(S)$, the design parameter's initial domain range (R), the elite ratio (r_e), and the number of bins (N_b).

8

Algorithm 1: A design parameter's information gain calculation

Input: A set of solutions S with known objective values $f(S)$, A design parameter's range R, Elite ratio r_e, Number of bins N_b

Output: Information gain γ and sub-intervals I of the design parameter

1   $e_0 \leftarrow -r \cdot \log_2(r) - (1-r) \cdot \log_2(1-r)$;   // Entropy assuming equally distributed elites

2   $e_w \leftarrow 0$;   // Initialized weighted entropy of the elites in S

3   $f_E = percentile(f(S), 1 - r_e)$;   // Threshold value of f for elite solutions

4   $S_E \leftarrow \{s \mid s \in S, f(s) \text{ is better than } f_E\}$;   // Elite solutions in S

5   $I \leftarrow$ make-equal-intervals(R, N_b);   // N_b equal bins from range R

6 **forall** $i \in I$ **do**

7      $p \leftarrow \frac{\|S_E \text{ in } i\|}{\|S \text{ in } i\|}$;   // Elite probability in sub-internal i

8      $e \leftarrow -p \cdot \log_2(p) - (1-p) \cdot \log_2(1-p)$;   // Information entropy of elites in i

9      $r \leftarrow \frac{\|S \text{ in } i\|}{\|S\|}$;   // Probability of input solutions S in i

10      $e_w \leftarrow e_w + e \cdot r$;   // Accumulated weighted entropy of elite distribution

11 $\gamma = e_0 - e_w$;   // Information gain is the decreased entropy

12 **return** γ, I;

Algorithm 1 first computes the baseline entropy (e_0), assuming an equal distribution of elite solutions across the parameter range. The algorithm determines the threshold value of f for elite solutions to identify the elite solutions (S_E). The initial range R is then decomposed into N_b equally spaced sub-intervals I. For each sub-interval i, the entropy of elites in i is calculated by the probability p of elite solutions. The algorithm also computes the probability r of input solutions S in each sub-interval, and accumulates the weighted entropy (e_w) by weighting the elite entropy with probability r before summing across sub-intervals. Finally, the information gain (γ) is computed as the difference between the baseline entropy (e_0) and the accumulated weighted entropy (e_w). A higher IG value for a design parameter indicates greater importance in reducing the uncertainty of finding the optimal solution within the search space.

Algorithm 2 and Figure 2 show the following steps, which converge design parameter intervals based on IG values, improving optimization efficiency by either converging interval ranges or fixing parameters as constants. Algorithm 2 takes as input the number of design parameters (n), corresponding initial domain range (R), corresponding information gains (Γ), and the corresponding sub-intervals (I). Additionally, it requires a set of elite solutions (S_E) and two ratios: r_{conv}, associated with the highest IG, which determines the subsets of parameters that should converge; and r_{const}, associated with the lowest IG, which defines the subsets of parameters that should be fixed to constants. Specifically, the lower threshold (γ_{conv}) of gain to converge is set at the (1 - r_{conv}) percentile of the information gains, while the upper threshold (γ_{const}) of gain to constant is set at the r_{const} percentile.

Algorithm 2: Refinement of design parameters' intervals based on information gains

Input: Number n of design parameters, Parameter ranges $R = \{R_1, R_2, \ldots, R_n\}$, Information gains $\Gamma = \{\gamma_0, \gamma_1, \ldots, \gamma_n\}$ and sub-intervals $\mathscr{I} = \{I_0, I_1, \ldots, I_n\}$ of the parameters from Algorithm 1, Elite solutions S_E, Ratio r_{conv} of design parameters to converge, Ratio r_{const} of design parameters to make constants

Output: Refined range intervals $R^* = \{R_1^*, R_2^*, \ldots, R_n^*\}$ for the n design parameters

```
1  γconv = percentile(Γ, 1 − rconv);              // Lower threshold of gain to converge
2  γconst = percentile(Γ, rconst);                // Upper threshold of gain to make constants
3  foreach i ∈ {0, 1, . . . , n} do
4      if γi ≥ γconv then
5          Ri* ← {r | r ∈ Ii, ∃v ∈ r, v appears in SE};   // Removing sub-intervals not in SE
6      else
7          if γi ≤ γconst then
8              constant ← get-design-param(optimum(SE), i);  // Get design value i in SE optimum
9              Ri* ← {constant};                     // Converged to the constant
10         else
11             Ri* ← Ri;                             // Not changed, otherwise
12 return R*;
```

For each design parameter, the algorithm applies a three-way decision rule based on its information gain (γ_i). If the gain γ_i is greater than or equal to γ_{conv}, the parameter range is converged by removing sub-intervals that do not appear in elite solutions. If the gain γ_i is less than or equal to γ_{const}, the parameter is converted to a constant value, which is determined as the design value observed in the optimum of elite solutions. Otherwise, the parameter range remains unchanged. Finally, the converged set of parameter ranges R^* is returned. This process effectively reduces the design search space by eliminating irrelevant or highly stable parameter variations, thereby improving the efficiency of the second-phase optimization.

3.1.5 Interpretable analysis of building design parameters and components

The IG-guided interpretable analysis starts with information from design parameters, traces their association with different design components, and finally provides stakeholders with guidance on overall design strategies. As shown in the Sankey diagram in Figure 3(a), design parameters originally belonging to various design components are ranked based on their IG values and subsequently categorized into three subsets, corresponding to different modes of domain interval convergence. Figure 3(b) further explains and visually presents the convergence modes within three IG-guided subsets. Furthermore, the IG values of individual design parameters can be aggregated to evaluate their associated design components, highlighting the most impactful components for design optimization within the given SBO task. The IG-guided interpretable analysis explicitly demonstrates the convergence to effective sub-intervals during the SBO process while effectively supporting designers and stakeholders in making informed design decisions.
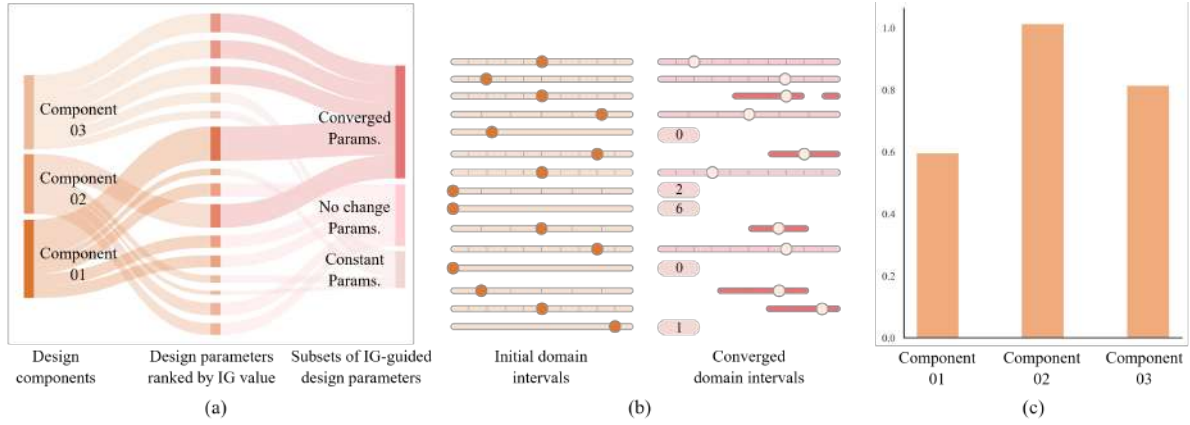
Figure 3. An example visualization for interpretable analysis in AIGGC. (a) Flow of design parameters information: from design components to IG-guided subsets. (b) Visual transformation from initial to converged domain intervals. (c) Illustration of IG ranking for design components.

3.2 Case study

To evaluate the robustness and scalability of the proposed method, we applied AIGGC to enhance three optimization algorithms to SBO tasks in two scales. The first conducted sustainable design optimization for energy efficiency at the building scale, while the other optimized daylight quality at the urban scale. Residential energy consumption has steadily risen in recent years, highlighting the need for sustainable building technologies (Qin & Pan 2020; Zhou & Xue 2023). Modular construction, known for its productivity, reusability, and pollution reduction, is extensively studied and particularly vital in Hong Kong due to its dense population and limited land resources (Zhou & Xue 2023). This paper optimizes the design of modular flats based on the building dimensions published by the Hong Kong Housing Authority (HKHA 2015). Given the floor layout of a one-bedroom modular flat, the building envelope was optimized to minimize energy consumption. Additionally, daylight quality, which significantly impacts residents' quality of life, is affected by mutual shading among urban buildings (Liu et al. 2023). Therefore, optimizing building forms during the early stages of urban block development is also essential for enhancing daylight accessibility and improving living conditions.

3.2.1 Definition of initial design parameters

The first design case focuses on optimizing the building envelope of a modular flat in Hong Kong, designed for 1-2 occupants, with an internal floor area rationalized to 14.1~14.5 m^2. Hong Kong has a subtropical climate, with warm and humid conditions year-round. Summers are long and hot, with dry-bulb temperatures exceeding 30°C, leading to a high energy demand for cooling (Zhou & Xue 2023). To enhance passive energy efficiency, we further optimize the envelope components. Numerous studies have identified the window-to-wall ratio (WWR) as a significant factor influencing building energy consumption (Wang et al. 2024). Besides, we consider details such as window shape (where variations in window height, given a fixed WWR, determine the window's width), sill height, and the angle and number of louvers used for

11

shading, as illustrated in Figure 4(a). The design scheme includes four façades to be optimized, comprising 11 continuous variables, 7 discrete variables, and 4 binary variables. The specific design parameters and their domain intervals are shown in Table 1.
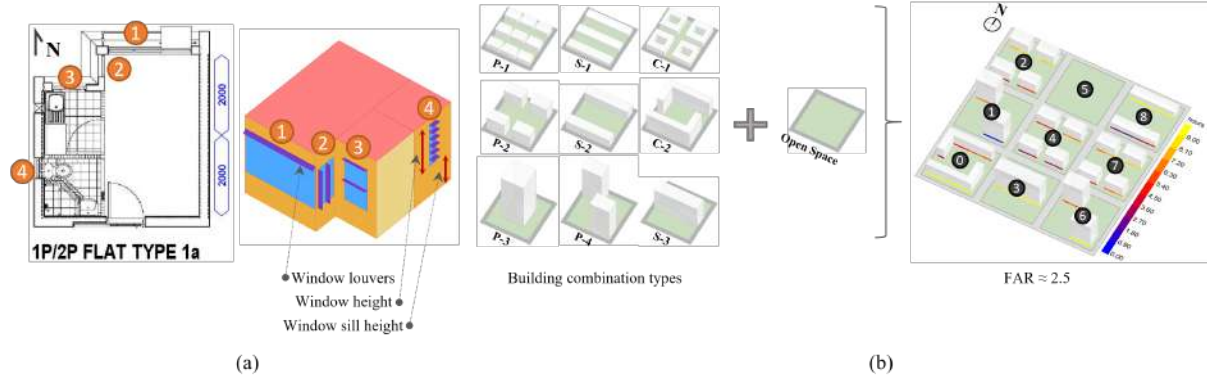

(a)   (b)

Figure 4. Design cases to be optimized. (a) Case 1: Envelope design optimization for one-bedroom modular flat; (b) Case 2: Urban block forms design optimization.

Table 1. Description of envelope design parameters for one-bedroom modular flat.

Design parameters	Parameter type	Unit	Parameter domain intervals	Precision
Window-to-Wall Ratio (WWR_1, WWR_2)	Continuous	-	$0.1 \leqslant WWR_1, WWR_2 \leqslant 0.6$	0.01
Window-to-Wall Ratio (WWR_3, WWR_4)	Continuous	-	$0.1 \leqslant WWR_3, WWR_4 \leqslant 0.3$	0.01
Window height ($WH_{1\&2}$)	Discrete	m	$1.0 \leqslant WH_{1\&2} \leqslant 2.0$	0.1
Window height (WH_3, WH_4)	Discrete	m	$1.0 \leqslant WH_3, WH_4 \leqslant 1.5$	0.1
Window sill height ($WSH_{1\&2}$, WSH_3, WSH_4)	Continuous	m	$0.80 \leqslant WSH_{1\&2}, WSH_3, WSH_4 \leqslant 1.20$	0.01
Window louvers count (LC_1, LC_2, LC_3, LC_4)	Discrete	-	$1 \leqslant LC_1, LC_2, LC_3, LC_4 \leqslant 6$	1
Window louvers angle (LA_1, LA_2, LA_3, LA_4)	Continuous	°	$-45 \leqslant LA_1, LA_2, LA_3, LA_4 \leqslant 45$	1
Window louvers direction (LVH_1, LVH_2, LVH_3, LVH_4)	Binary	-	Horizontal = 0; Vertical = 1	-

The second design case focuses on optimizing the building forms of urban blocks in Jianhu City, located in Jiangsu Province, China. The selection of initial design parameters is based on the findings of Liu et al. (2023). As shown in Figure 4(b), the urban block consists of nine zones, numbered from 0 to 8. According to the generative rules by Liu et al., one of these zones is designated as open space, while the remaining eight plots are selected from nine typical building combinations. These building combinations are derived from actual residential clusters in Jianhu City and are categorized into three major types: point-type buildings (including P-1, P-2, P-3, and P-4), slab-type buildings (including S-1, S-2, S-3), and courtyard-type buildings (including C-1 and C-2). Specifically, P-1, S-1, and C-1 are low-rise buildings; P-2, S-2, and C-2 are mid-rise buildings; P-3, P-4, and S-3 are high-rise buildings; with their respective floor number counts detailed in Table 2. Each block is uniformly south-facing, with a floor area ratio (FAR) of approximately 2.5. There are 1 discrete variable, 9 continuous variables, and 8 categorical variables.

12

Table 2. Description of urban block form design parameters.

Design parameters	Parameter type	Unit	Parameter domain intervals	Precision
Open space location (*OPos*)	Discrete	-	[0, 1, 2, 3, 4, 5, 6, 7, 8]	1
Building type of remaining plots (*Pos*$_1$, *Pos*$_2$, *Pos*$_3$, *Pos*$_4$, *Pos*$_5$, *Pos*$_6$, *Pos*$_7$, *Pos*$_8$)	Categorical	-	[P-1, S-1, C-1, P-2, S-2, C-2, P-3, P-4, S-3]	-
Number of floors (*NF*$_{P1}$, *NF*$_{S1}$, *NF*$_{C1}$, *NF*$_{P2}$, *NF*$_{S2}$, *NF*$_{C2}$, *NF*$_{P3}$, *NF*$_{P4}$, *NF*$_{S3}$)	Continuous	-	$1 \leqslant NF_{P1}, NF_{S1}, NF_{C1} \leqslant 3$ $4 \leqslant NF_{P2}, NF_{S2}, NF_{C2} \leqslant 12$ $13 \leqslant NF_{P3}, NF_{P4}, NF_{S3} \leqslant 30$	1

3.2.2 Definition of objective functions

In the first design case, we aim to minimize energy use intensity and the objective function can be concluded as:

$$\mathbf{arg\ min}_{x \in X}\, EUI(x) \qquad\qquad (1)$$

Where *EUI* is the energy use intensity (kWh/m^2·yr) that can be calculated by dividing the total annual energy consumption over the gross floor area (Konis et al. 2016), *x* represents a combination of the *n* design parameters ($x_1, x_2, ..., x_n$), and *X* indicates the set of all potential design combinations. The optimization problem's dimensionality is defined by *n*, determining the search space complexity and computational effort. The numerical computing of *EUI* is performed using the *Honeybee* components in the *Grasshopper* platform (Zhou & Xue 2023). First, the *Honeybee-Radiance* (*Ver.1.5*) component integrates context data (Qin & Pan 2020), including local climate, construction materials, construction type, and HVAC systems, to simulate annual daylight based on a predefined grid size (G$_{s1}$). The results are then utilized to set up the daylight control schedule for the target model. Next, the context data and the generated schedule are passed to the *Honeybee-OpenStudio* (*Ver.1.5*) component, which translates this information to create an energy model (.osm) and convert it into a .idf file for total *EUI* calculation via the built-in *EnergyPlus* program (Roudsari & Pak 2013). According to Qin and Pan (2020), the *EUI* of local modular flats in Hong Kong is generally 153.8 kWh/m^2·yr.

In contrast, the second design case focuses on an opposing optimization objective: maximizing the average direct sunlight hours on the south-facing ground floors of urban blocks in Jianhu City. Jianhu City is situated in the hot summer and cold winter (HSCW) climate zone. According to mainland China's building code (MOHURD 2018), residential buildings in this zone must receive at least two hours of sunlight on the south-facing ground floor on the coldest day of the year, i.e., January 20th (Liu et al. 2023). We formulate the function as follows:

$$\mathbf{arg\ max}_{y \in Y}\, \frac{1}{m} \sum_{i=1}^{m} DSH_i(y) \qquad\qquad (2)$$
$$\mathbf{subject\ to}\ |\,\mathrm{FAR_{ori}} - FAR_{opt}\,| \leqslant 0.05$$

Where $DSH_i(y)$ is the direct sunlight hours for the *i*-th sampling point as a function of the design parameter *y*, *m* means the total number of sampling points determined by the simulation grid size (G$_{s2}$), and *Y* denotes the set of all design parameters. The constraint is that the absolute difference between the optimized block's floor area ratio (FAR_{opt}) and the original block's FAR (FAR$_{ori}$ = 2.5) must be less than 0.05. The $DSH_i(y)$ can be simulated through

the *Ladybug-Direct Sun Hours* (*Ver.1.5*) component, which calculates direct sunlight hours on geometry using sun vectors and ray intersection methods (Roudsari & Pak 2013).

3.2.3 Optimization algorithms selection

In this study, both design cases are single-objective optimization tasks. To evaluate the robustness of the proposed method, we compared three optimization algorithms with distinct search strategies, GA, CMA-ES, and RBFOpt, which are integrated into *Grasshopper* and interact smoothly with the design parameters and simulation engines. Statistical data indicates that GA has been the most frequently used algorithm in single-objective SBO tasks over decades (Evins 2013; Nguyen et al. 2014). Moreover, CMA-ES and RBFOpt have demonstrated efficiency advantages in black-box optimization for sustainable building design (Kämpf et al. 2010; Xue et al. 2019; Wortmann 2019; Rehbach et al. 2022).

GA is a population-based metaheuristic algorithm inspired by natural selection, iteratively generating new populations through selection, mutation, and crossover (Katoch et al. 2021). CMA-ES aims to reduce the stochastic nature of evolutionary strategies by using the Covariance Matrix (CM) in each iteration, which has been shown to be an efficient method in building design optimization, especially for small population sizes (Hansen et al. 2003; Ramallo-González & Coley 2014). RBFOpt is a model-based algorithm that applies sampling points to refine an approximation model for the unknown objective function (Waibel et al. 2019). GA can be implemented in the *Galapagos* plugin, while CMA-ES and RBFOpt can be operated in the *Opossum* plugin.

4 Experimental tests

4.1 Experimental settings

The experiments were conducted on a desktop computer with an Intel (R) Core i7-10700 CPU @ 2.90 GHz processor and 32 GB memory. In this study, both design cases were parametrically reconstructed in *Rhinoceros3D* (*Ver.7.0*) and the visual programming platform *Grasshopper*, based on the detailed dimensions provided by the Hong Kong Housing Authority (HKHA 2015) and the published work of Liu et al. (2023), respectively.

The first sustainable design case utilized the *Ladybug-EPWmap* (*Ver.1.5*) component to obtain meteorological data for Hong Kong (ASHRAE 2021). The *Honeybee* plugin assigned physical properties of construction materials to the parametric model, including thickness, conductivity, density, specific heat capacity, and U-value, following (Qin & Pan 2020). The *EUI* value was then calculated via the *Honeybee-Radiance* (*Ver.1.5*) and *Honeybee-OpenStudio* (*Ver.1.5*) components, with a sensor grid size (G_{s1}) of 0.2 meters. The original one-bedroom modular flat served as the baseline, with its design parameters used as initial optimization inputs, resulting in an *EUI* value of 159.599 kWh/m^2·yr, as detailed in Table 1 in the Appendix.

Similarly, in the second sustainable design case, climate data for Jianhu City was collected using the *Ladybug-EPWmap* (*Ver.1.5*) component and processed through the *Ladybug-SunPath* (*Ver.1.5*) component to obtain the sun position between 8:00 a.m. and 5:00

p.m. on January 20th (i.e., the coldest day). The resulting sunlight vector data was then fed into the *Ladybug-Direct Sun Hours* (*Ver.1.5*) component to calculate the direct sunlight duration on the ground floor of a south-facing urban block. The sensor grid size (G_{s2}) was set to 1 meter for this urban-scale optimization. The baseline urban model's parameters are listed in Table 2 of the Appendix, with a corresponding *DSH* value of 6.081 hours.

This experiment evaluated the robustness and advantages of the AIGGC method across two design cases using different SBO algorithms, i.e., RBFOpt, CMA-ES, and GA. Since many algorithms contain randomized factors during the optimization process (Waibel et al. 2019), each algorithm was rerun 5 times for Case 1 (as a single set of runs required 36 hours) and 20 times for Case 2 to ensure reliable results.
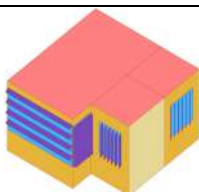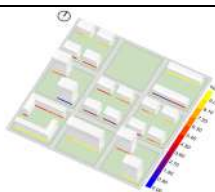
For the three SBO algorithms, this experiment included an experimental group with AIGGC and a control group without AIGGC under the same iteration budget. The detailed hyperparameter settings for the single-objective algorithms are described in Appendix Table 3, referring to previous literature (Waibel et al. 2019). For both design cases, the total iteration budget (N) was set to 300 with a distribution ratio (r_d) of 1:2, resulting in the pre-convergence budget (N_1) as 100 and the post-convergence budget (N_2) as 200. The elite ratio (r_e) was set to 20% to classify the solutions into 'elite' and 'non-elite' groups. The partitioning method for sub-interval bins was chosen as BinM (N_b) = 10, which divided each design parameter domain into 10 bins. For design parameters convergence, r_{conv} and r_{const} were both set to one-third.

4.2 Experimental results and analysis

4.2.1 Optimized results with AIGGC

The experimental results compare the best of optimized design solutions from multiple runs of the three SBO algorithms (i.e., RBFOpt, CMAES, and GA), using the AIGGC method, against the baseline design solution, as detailed in Table 3. RBFOpt, after five reruns of three SBO algorithms, provided the best optimization result in Case 1, resulting in a minimum *EUI* value of 149.149 kWh/m²·yr. Compared to the baseline design solution, all four window façades showed a significant increase in the number of louvers. Notably, except for the first window, the remaining three featured a vertical louver design.

Table 3. Comparison between the best of optimized solutions with AIGGC and the baseline solution.

	Best optimized solution based on AIGGC	Baseline design solution		Best optimized solution based on AIGGC	Baseline design solution
Case 1			Case 2		
EUI (kWh/m²·yr)	149.149	159.599	*DSH* (hours)	9.000	6.081
Algorithm	RBFOpt		Algorithm	RBFOpt	

15

In Case 2, RBFOpt still stands out among the other algorithms across 20 reruns, achieving the optimal *DSH* value of 9 hours under the constraints of a given floor area ratio. The P-1 building cluster most frequently appeared in the best solution from multiple runs, with a noticeable trend of locating lower-rise blocks in the southern plots and higher-rise buildings in the northern plots.

4.2.2 Robustness and significance across different optimization algorithms

Table 4 compares the average and best objective performance values among three SBO algorithms between the experimental group (With AIGGC) and the control group (NO AIGGC), as well as the magnitude and significance of performance improvements achieved by AIGGC. The result demonstrates that incorporating AIGGC into SBO algorithms consistently improves optimization performance across multiple runs, with statistically significant enhancements in average results. Notably, RBFOpt shows the best overall performance among all algorithms, achieving the best solution in both cases.

Table 4. The magnitude and significance of AIGGC's performance in improving SBO algorithms in multiple runs.

Case	Objective function f^* (Baseline value v_0)	SBO algorithm	Average SBO results					Best solution		
			NO AIGGC	With AIGGC	Δ	% Imp.[†]	Sig.[#]	NO AIGGC	With AIGGC	Δ
1	**min** *EUI* (159.599 kWh/m²·yr)	RBFOpt	150.289	**149.301**	-0.988	0.62	**0.008**	149.719	**149.149**	-0.57
		CMA-ES	151.961	150.935	-1.026	0.64	**0.019**	151.429	150.099	-1.33
		GA	155.305	154.241	-1.064	0.67	**0.018**	154.469	153.709	-0.76
2	**max** *DSH* (6.081 hours)	RBFOpt	8.449	**8.579**	0.13	2.14	**0.036**	8.764	9	0.236
		CMA-ES	7.997	8.202	0.205	3.37	**0.037**	8.554	8.708	0.154
		GA	7.977	8.265	0.288	4.74	**0.000**	8.329	8.680	0.351

*: Smaller values are better for Case 1 and larger values are preferred for Case 2.
†: Improvement by percentage, $|\Delta|/v_0 \times 100\%$, v_0 for baseline value.
#: Two-tailed p-value of independent t-test, bold when p-value < 0.05.

In Case 1, where a lower *EUI* value is preferred, AIGGC leads to a reduction in the average *EUI* across all algorithms, with the improvement percentage ranging from 0.62% to 0.67%. With the incorporation of AIGGC, RBFOpt reduced the average *EUI* from 150.289 kWh/m²·yr (NO AIGGC) to 149.301 kWh/m²·yr. CMA-ES and GA also showed improvements with AIGGC, achieving average *EUI* reductions of 0.64% (from 151.961 to 150.935 kWh/m²·yr) and 0.67% (from 155.305 to 154.241 kWh/m²·yr), respectively. Moreover, RBFOpt achieved the best performance value of 149.149 kWh/m²·yr after five reruns, representing a 3.024% improvement compared to the general *EUI* of local modular flats, which is 153.8 kWh/m²·yr.

In Case 2, where higher *DSH* values are desirable, AIGGC similarly enhances the performance of all three algorithms, with the improvement percentage ranging from 2.14% to 4.74% across 20 repeated runs. When combined with AIGGC, RBFOpt achieved an average *DSH* of 8.579 hours, which is 0.13 hours higher than without AIGGC. Similarly, CMA-ES and GA showed notable enhancements with AIGGC, achieving average sunlight hours improvements of 3.37% (from 7.997 to 8.202 hours) and 4.74% (from 7.977 to 8.265 hours), respectively. The best *DSH* value obtained with AIGGC was 9.000 hours, followed by 8.708

16

hours identified by CMA-ES and 8.680 hours identified by GA, all significantly exceeding the two-hour requirement specified in the local residential building code.

The statistical significance of the performance improvements was evaluated using the independent two-tailed t-test. For both cases, RBFOpt consistently showed significant improvements when AIGGC was applied (two-tailed $p = 0.008 < 0.05$ for Case 1 and $p = 0.036 < 0.05$ for Case 2). The significant p-values across all algorithms validate the robustness and reliability of the AIGGC method, demonstrating its ability to improve optimization performance under different objectives and scenarios.

Figure 5 (a) and (b) apply violin plots to compare the deviations of best performance values achieved by three SBO algorithms under two conditions. The 'NO AIGGC' control group is represented in blue, the 'AIGGC' experimental group is in red, and the baseline is indicated by a red dashed line. In both cases, the median values of the 'AIGGC' group consistently outperform those of the 'NO AIGGC' group, with the 'AIGGC' group showing a larger overall deviation from the baseline, indicating a more significant improvement. Overall, the RBFOpt algorithm with the AIGGC method exhibits the most concentrated distribution and is more efficient in finding the minimum solution for *EUI* and the maximum solution for *DSH*.
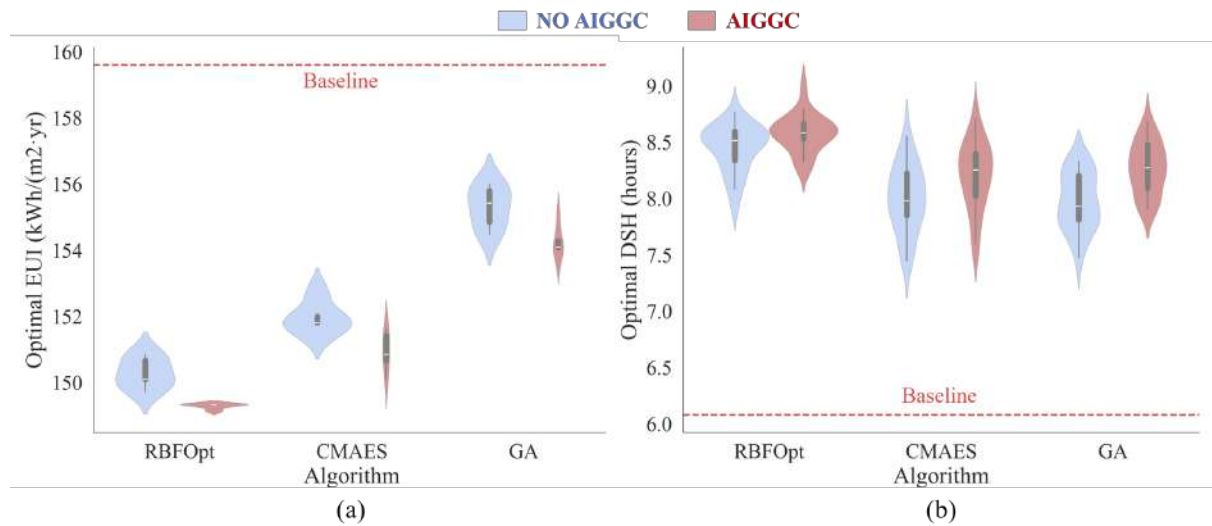
Figure 5. Comparison of optimal performance deviations of three optimization algorithms with and without AIGGC. (a) Case 1: Minimize *EUI*; (b) Case 2: Maximize *DSH*.
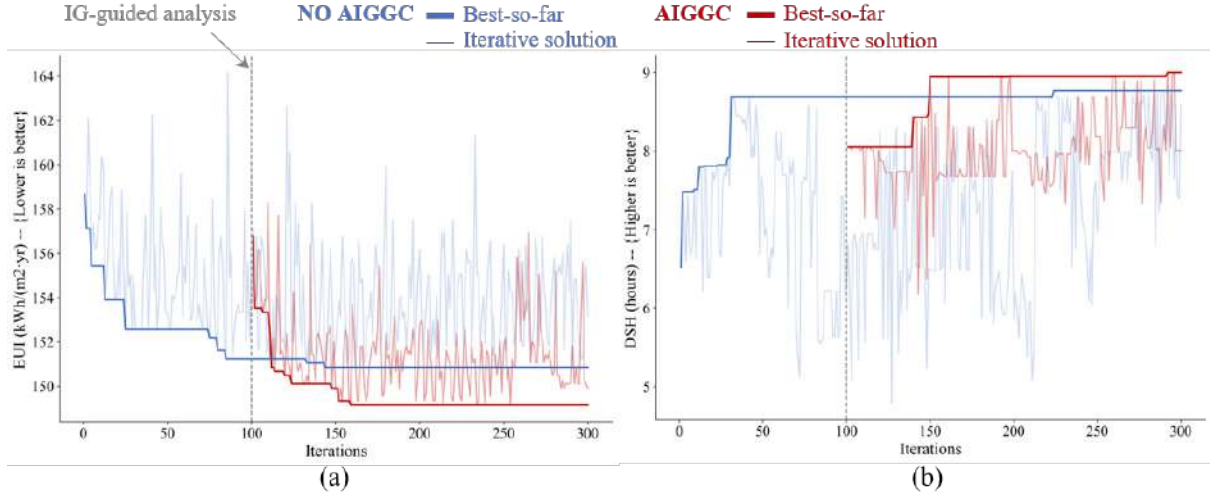
Figure 6. Convergence trend of optimization with and without AIGGC. (a) Case 1: Minimize *EUI*; (b) Case 2: Maximize *DSH*.

Figure 6 (a) and (b) illustrate the optimization line graphs of RBFOpt achieving the best performance in two cases, i.e., 149.149 kWh/m^2·yr for Case 1 and 9.000 hours for Case 2. The convergence trends highlight the performance improvements achieved by integrating the AIGGC method. The blue lines represent the control group without AIGGC, while the red lines represent the experimental group with AIGGC. The thin solid lines depict the iterative solution values during the optimization process, and the thick solid lines indicate the best objective values achieved so far. It can be observed that in high-dimensional optimization problems, algorithms without AIGGC struggle to converge in the later stages and often get trapped near sub-optimal solutions. In contrast, optimization algorithms incorporating AIGGC can apply IG-guided information to identify superior solutions. According to the experimental settings, the group with AIGGC first used 100 iterations to compute a dataset, followed by IG-guided analysis and refining of the design parameters. The results demonstrate that the experimental group, with converged design parameters, quickly surpassed the control group within the 50 iterations in the second phase, while the control group ran for 150 iterations. Statistically, AIGGC performed a faster descent/ascent in Figure 6. The fast descent/ascent confirms the hypothesis that reducing the dimensionality of the design search space enhances the efficiency of the RBFOpt algorithm.

4.2.3 Design parameters and components analysis

Figures 7 and 8 illustrate the reduction in the number of design parameters and the size of the potential solution space before and after IG-guided analysis for both cases. In Case 1, the initial four design components included 22 design parameters, with a fine-grained division of the total domain intervals revealing 4.45×10^{25} possible solutions. After applying the AIGGC method to calculate, rank, and group the IG value for each design parameter, the number of design parameters was reduced to 16, with 8 partially converged and 8 remaining unchanged. Consequently, the design solution space size decreased sharply to 6.30×10^{18}, by seven orders of magnitude. Similarly, in Case 2, the design parameters were reduced from 18 to 12, with 6

18

partially converged and 6 unchanged, while the solution space shrank from 4.45×10^{16} to 2.21×10^9 by seven orders of magnitude.
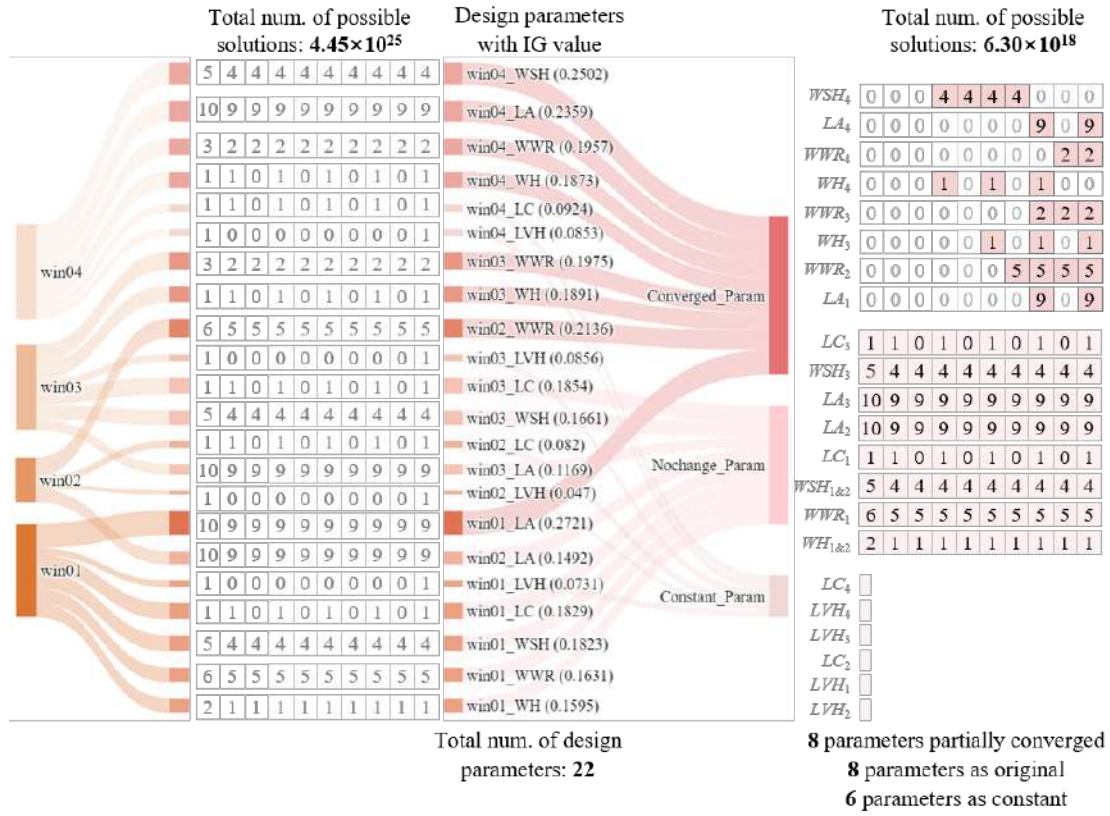

Figure 7. Detailed visualization of the design parameter convergence process for RBFOpt's best performance solution in Case 1.
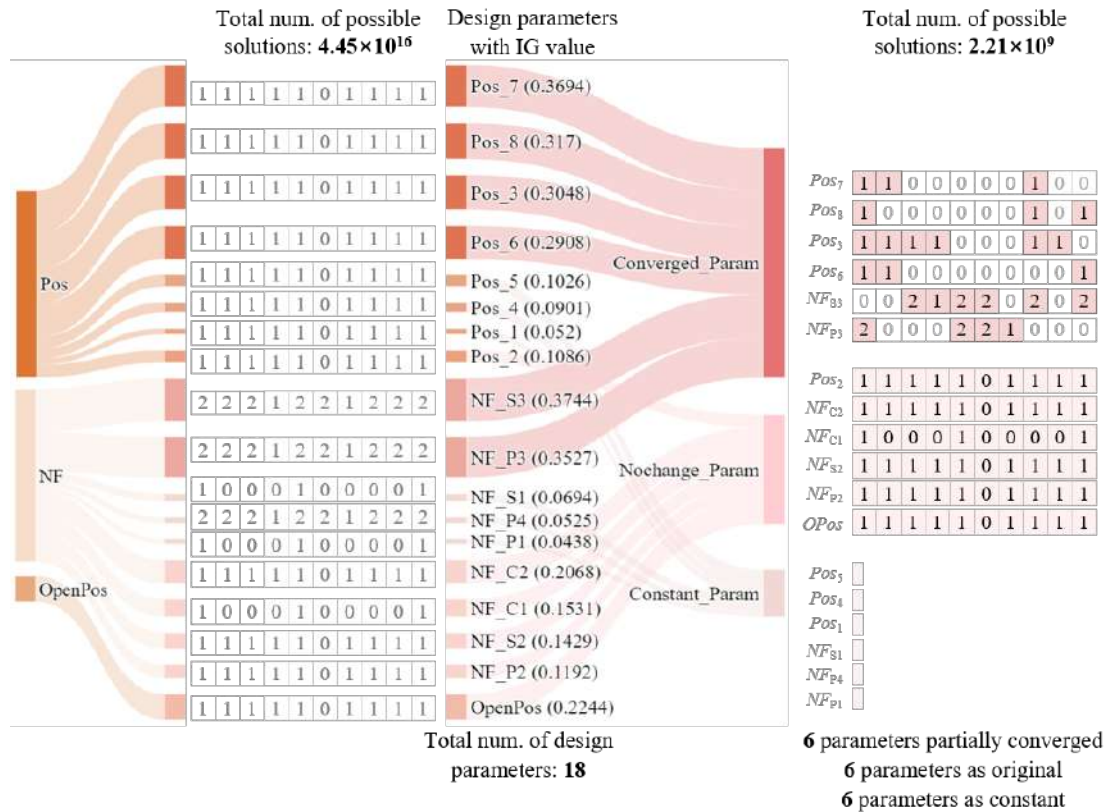

19

Figure 8. Detailed visualization of the design parameter convergence process for RBFOpt's best performance solution in Case 2.

Figure 9 presents a series of heatmaps visualizing the average probability associated with the sub-interval bins of each design parameter. The probability indicates the likelihood of solutions within a given bin belonging to the 'elite' group. The color intensity of the heatmap reflects the probability magnitude, with darker colors corresponding to higher probabilities. Blank regions denote that there are no design solutions within those sub-interval bins. The bin sequence is arranged from 1 to 10, representing the full domain range of each design parameter from smallest to largest. On the right side, a bar chart illustrates the average IG value of each design parameter observed in this experiment.
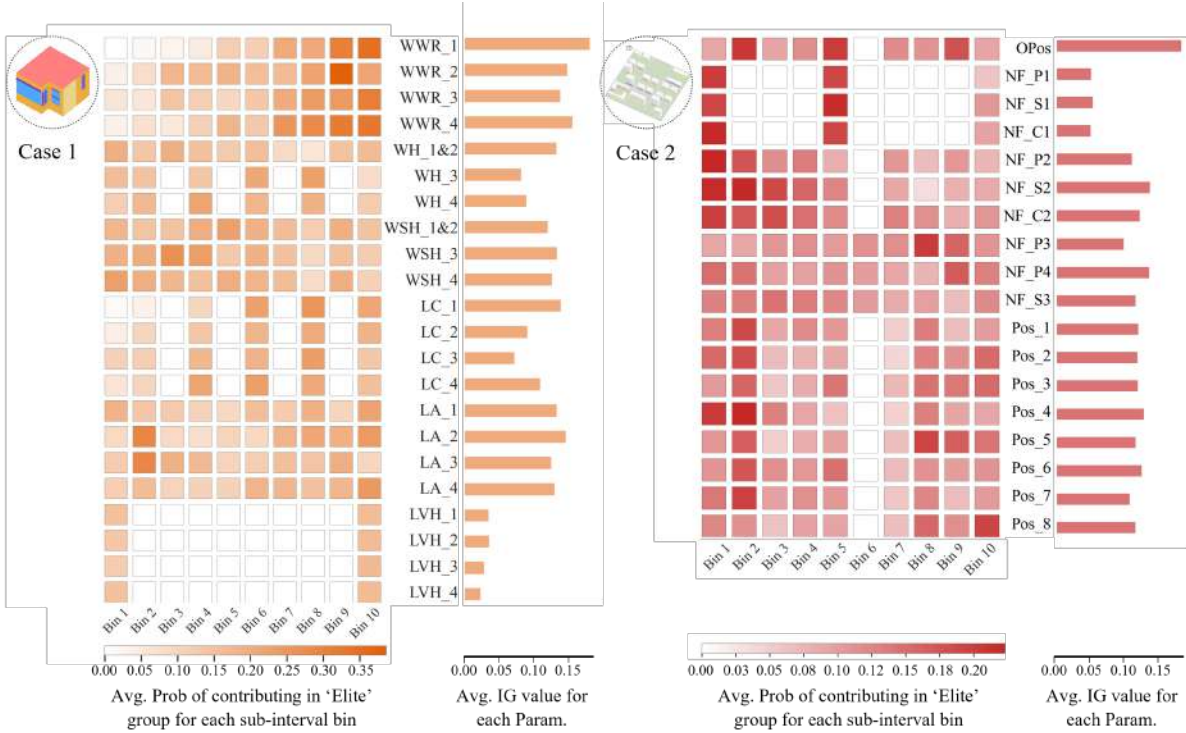
Figure 9. Visualization of design parameters' average IG values and probabilities of sub-interval bin contributions to the 'elite' group.

In Case 1, the window-to-wall ratio (*WWR*) and window louvers' angle (*LA*) exhibit relatively high IG values overall, with WWR_1 showing the highest average IG value. The results suggest that decision-makers may focus on adjusting the values of *WWR* and *LA* to minimize energy use intensity efficiently. Moreover, high-probability sub-intervals for *WWR* are concentrated in the larger bin indices (i.e., bins 9th and 10th), which means that when the *WWR* of façades 1 and 2 approaches 0.5 to 0.6, and that of façades 3 and 4 approaches 0.27 to 0.3, the likelihood of achieving low-*EUI* design solutions increases. Similarly, for LA_2, the 2nd bin emerges as a promising sub-interval, suggesting that setting LA_2 between -35° and -27° is more effective for high-performance building design exploration. In contrast, the parameter *LVH* contributes minimally to the optimization objective regarding IG value and probability.

In Case 2, *OPos* shows the highest average IG value, with higher probabilities of approaching high-*DSH* solutions concentrated in sub-interval bins 2nd, 5th, and 9th,

20

corresponding to plots 1st, 4th, and 7th in the urban block design. For building clusters of P-1, S-1, and C-1, the suggested number of floors is primarily concentrated in the 1st and 2nd bins, indicating single- or double-story configurations. Moreover, for clusters P-2, S-2, and C-2, higher probabilities of optimal solutions are found from bins 1st to 3rd, with a preferred range of four to six floors. And the suggested floor numbers for P-3, P-4, and S-3 building clusters are 25–26, 27–28, and 17–18, respectively. Regarding plot allocation, S-1 is applicable for most plots, whereas C-2 presents a lower likelihood of existing good design solutions across all plots. P-1 and S-3 are recommended for plots 4th and 8th, respectively.

Analyzing the IG values of design components is also meaningful, as it highlights their importance in reducing the uncertainty of finding optimal solutions within the optimization search space. Figure 10(a) and (b) compare the average IG values of design components and parameter categories in Case 1. Specifically, Win_{01} demonstrates the highest IG value (0.75), followed by Win_{02} (0.699). Therefore, decision-makers may prioritize the optimization of Win_{01} to effectively reduce building energy consumption. Among the five parameter categories, *WWR* ranks the highest with an IG value of 0.624, while *LVH* ranks the lowest with an IG value of 0.118. The result means that *WWR* is the most significant factor in the Case 1 optimization task, whereas *LVH* can be given less emphasis.
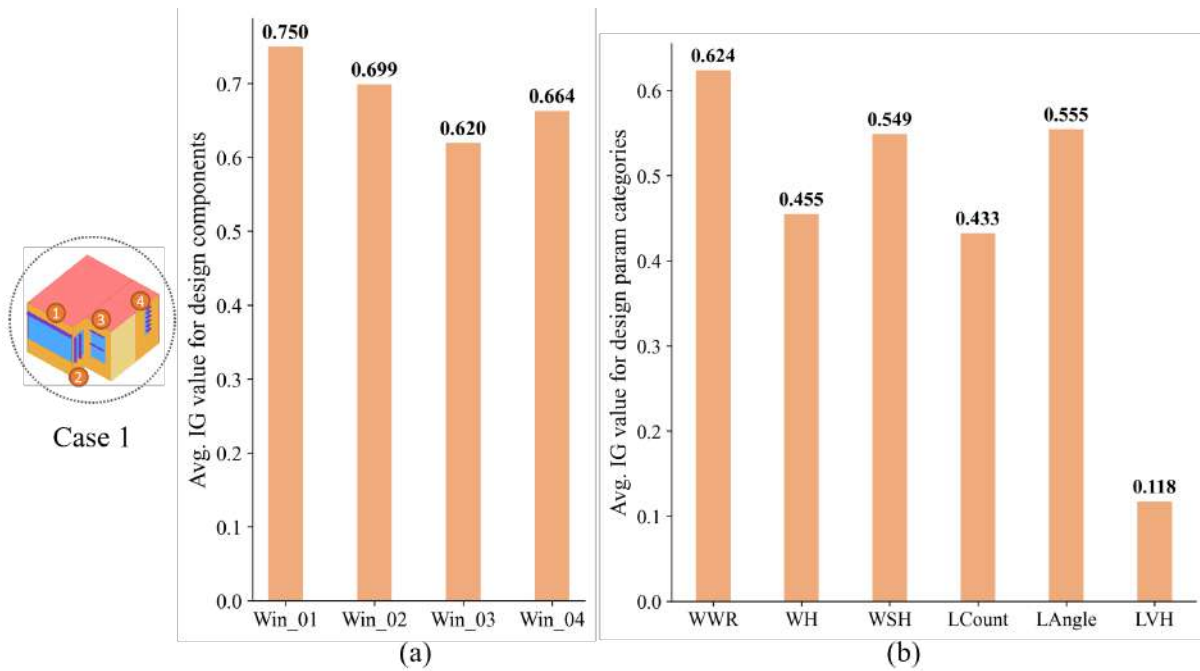

Figure 10. Visualization of average IG values for design components and parameter categories in Case 1. (a) Average IG values for design components; (b) Average IG values for design parameter categories.

Similarly, in Case 2, the placement of the 'Open Space' plot significantly impacts the average direct sunlight hours on the south-facing ground floors of urban blocks. Combining Figures 9 and 11, the three plots with the highest average IG values also correspond to the plots with the highest probabilities, i.e., plot 1st (IG of 0.327), plot 4th (IG of 0.371), and plot 7th (IG

of 0.349). This observation suggests that positioning the 'Open Space' plot along the central axis of the urban block is most conducive to achieving the optimal solutions.
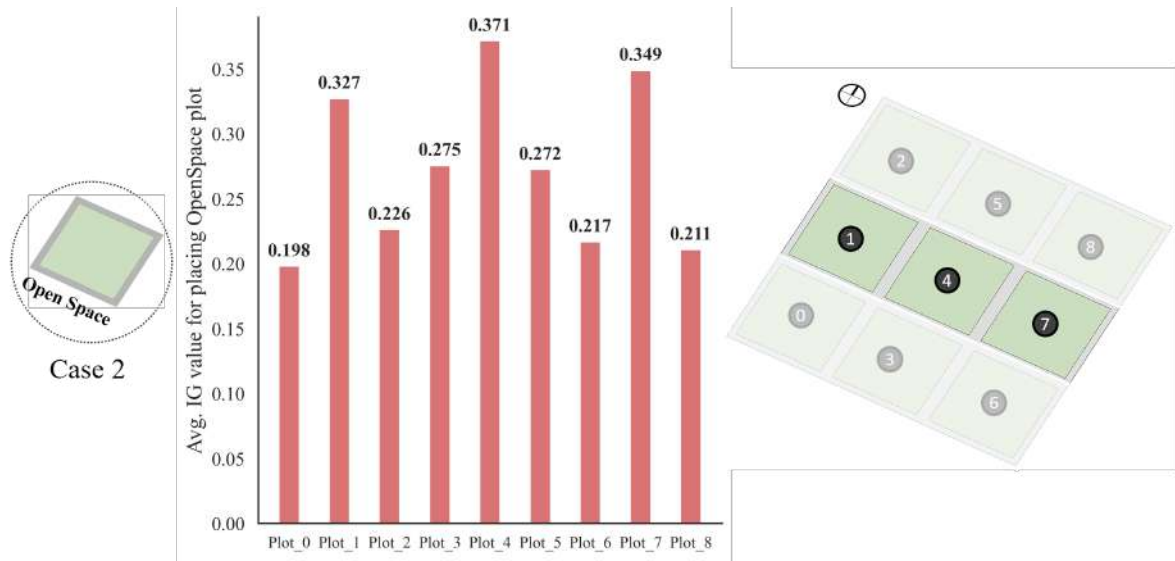

Figure 11. Visualization of average IG values for positioning 'Open Space' plot in Case 2.

4.3 Sensitivity analysis

A sensitivity analysis was conducted to determine the trade-off between time cost and optimal results, identifying the most effective experimental settings for the experimental and control groups. This experiment involved three key parameters: (i) the total iteration budget (N), with comparisons made between 100, 300, 500, 1000, 3000, and 5000; (ii) the distribution ratio (r_d) between the two optimization phases, tested with ratios of 1:1, 1:2, and 1:4; and (iii) the partitioning method for sub-interval bins (BinM), which was evaluated using three scenarios: BinM = 10, BinM = $N_1/10$, and BinM = $\sqrt{N_1}$. Due to the computational expense of energy consumption simulations in Case 1, Case 2 was selected for comparing experimental configurations. The experimental and control groups were compared under the same iteration budget.

Figures 12 and 13 visually compare the impact of different experimental configurations on the number of sub-interval bins and the maximum *DSH* values achieved via the AIGGC method. Where BinM is distinguished by symbols and colors: blue squares represent 'BinM = $N_1/10$', purple inverted triangles for 'BinM = $\sqrt{N_1}$', and red circles for 'BinM = 10'. Meanwhile, solid symbols indicate that the experimental group outperformed the control group (i.e., obtained higher *DSH* values), while hollow symbols indicate the opposite. In addition, the distribution ratio (r_d) is represented by pink circles of varying sizes.
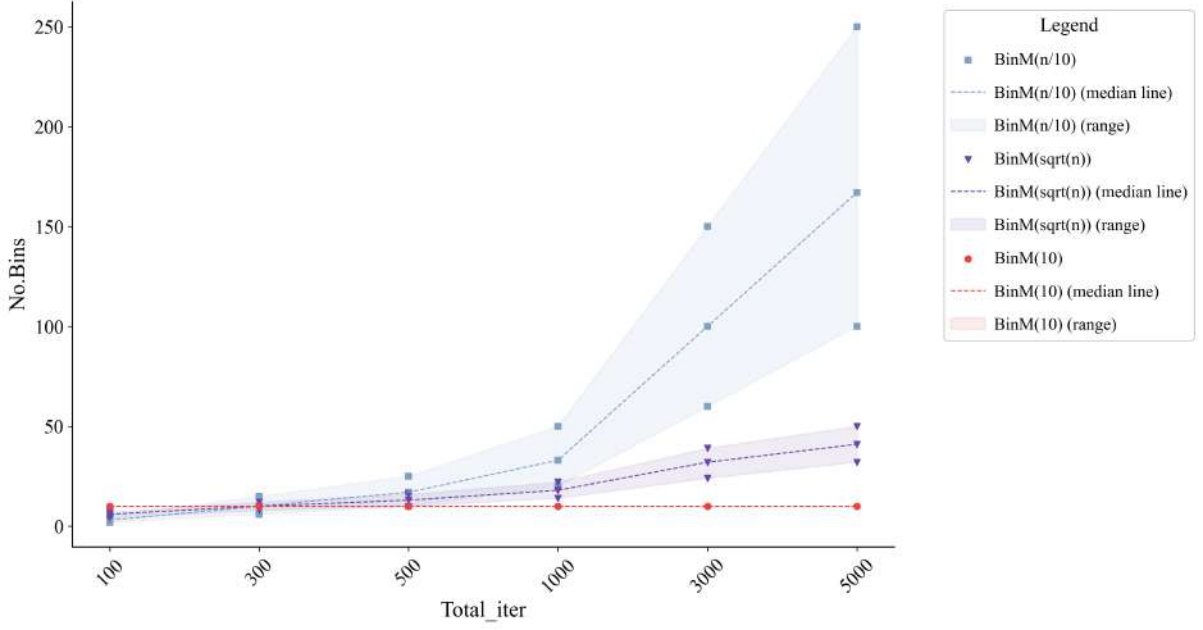
Figure 12. Variation in bin counts for BinM methods across iteration budgets.
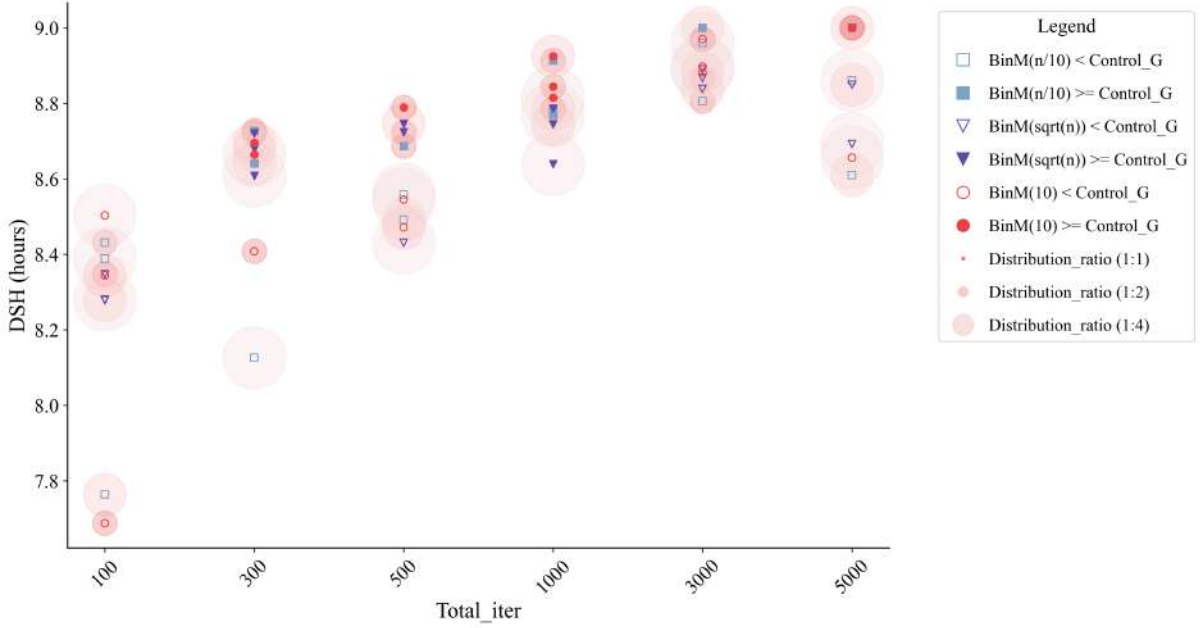

Figure 13. Sensitivity analysis of experimental settings.

From Figures 12 and 13, it can be observed that the number of sub-interval bins increases significantly with higher iteration budgets at 'BinM = N_1/10', indicating finer granularity for IG-guided analysis. When 'BinM = N_1/10', the frequency of finding the optimal solution is also higher under most iteration budgets. Interestingly, with 'BinM = 10', the number of bins remains constant regardless of the iteration budget, yet it consistently ensures the discovery of optimal solutions (e.g., performing well with budgets of 300, 500, 1000, and 5000). In contrast, 'BinM = $\sqrt{N_1}$' shows relatively average performance. Furthermore, a side-by-side comparison in Figure 12 reveals that a distribution ratio (r_d) of 1:2 is most common near the top of the stack of points, implying a higher chance of finding the optimal solution.

23

The proportion of solid and hollow symbols is also noteworthy. Only hollow symbols are observed at a total iteration budget of 100, indicating that the generic SBO process is more suitable for small-budget optimization tasks. In medium-budget tasks (ranging from 300 to 1000 iterations), the AIGGC method demonstrates clear advantages, particularly at 1000 iterations, where it consistently outperforms the generic SBO across all experimental configurations. For large-budget tasks (e.g., 3000 and 5000 iterations), the AIGGC method demonstrates a more remarkable ability to find the optimal solution than the generic SBO, as solid symbols consistently appear at the top.

In this study, considering the balance between the time cost of expensive simulations (e.g., energy simulation) and overall efficiency, we recommend the experimental configuration of 'BinM = 10', a distribution ratio (r_d) of 1:2, and a total iteration budget of 300.

5 Discussion

This study presents the AIGGC method for high-dimensional SBO building designs for the first time, establishing an information-theory-based method for the automatic convergence of design parameter domains, thus reducing the dimensionality of the search space. Based on the dataset from first-phase optimization, the AIGGC method effectively enhances the performance of existing optimization algorithms under a limited iteration budget. Through IG-guided fine-grained visual analysis at the parameter and component levels, Case 1 highlights the importance of the Win_01 object and the design parameter category *WWR*, while Case 2 provides applicable insights into the central axis placement of the 'Open Space' plot. AIGGC applies information gain measurement into interpretable guidance, to enable designers and stakeholders to identify optimization strategies and make informed decisions in early design exploration. It can also enhance SBO efficiency in real-world sustainable building projects while improving stakeholders' understanding of optimization convergence.

Nevertheless, this study still has a few limitations. First, the analysis of design parameters was conducted independently based on information gain, while potential non-linear and complex interactions between parameters remain an area for future exploration. Second, future research will consider more complex real-world projects, incorporating factors such as practical occupant schedules, energy-efficient building materials, and the shading effects or microclimate conditions of the built environment to optimize thermal comfort and energy consumption, further assessing the method's scalability to multi-objective optimization tasks. Third, future work will focus on dynamically enhancing search efficiency within the solution space by integrating advanced machine learning models and extending the applications to high-dimensional optimization problems in other fields, such as architectural engineering and environmental science.

6 Conclusion

The proposed Automatic Information Gain-guided Convergence (AIGGC) method in this paper demonstrates promising experimental results in enhancing effectiveness and

24

interpretability for high-dimensional sustainable building designs. The AIGGC method reallocates a limited budget by utilizing first-phase optimization results as a dataset and performing IG-guided analysis on sub-intervals of each design parameter. The value of information gain assists stakeholders in quickly identifying high-information design parameters and high-quality domain intervals. The interpretable analysis of building design parameters and components enables stakeholders to converge design parameters by effectively reducing the number of design parameters as well as the size of the potential solution space. This study validated the AIGGC method for robustness and scalability in optimizing energy consumption and daylight quality at both the building and urban scales, while also significantly improving the convergence efficiency of three SBO algorithms — RBFOpt, CMA-ES, and GA.

The findings in this study contribute to both the theory and application of SBO in high-dimensional architectural design involving a large number of design parameters. The AIGGC method establishes an information-theory-based method for optimizing design parameters in addressing the challenge of the 'curse of dimensionality' in design search spaces. Furthermore, for non-derivative black-box SBO tasks, this method can enhance optimization efficiency while integrating interpretability analysis, enabling building designers and stakeholders to make informed and rational decisions in early architectural design exploration.

Future work directions include multivariate analysis of design parameters, integration of IG-based metrics with advanced machine learning techniques to uncover non-linear correlations, and exploration of AIGGC's applications in broader fields, such as multi-objective optimization in engineering and environmental science.

Acknowledgment

References

ASHRAE. (2021). *Weather Data Viewer.* Peachtree Corners, GA, USA: American Society of Heating, Refrigerating and Air-Conditioning Engineers. Retrieved 12 8, 2024, from https://www.ashrae.org/technical-resources/bookstore/weather-data-center#weather

Brown, N. C. & Mueller, C. T. (2019). Design variable analysis and generation for performance-based parametric modeling in architecture. *International Journal of Architectural Computing, 17*(1), 36–52. doi:10.1177/1478077118799491

Bushra, N. (2022). A comprehensive analysis of parametric design approaches for solar integration with buildings: A literature review. *Renewable and Sustainable Energy Reviews, 168*, 112849. doi:10.1016/j.rser.2022.112849

Chen, S., Montgomery, J. & Bolufé-Röhler, A. (2015). Measuring the curse of dimensionality and its effects on particle swarm optimization and differential evolution. *Applied Intelligence, 42*, 514–526. doi:10.1007/s10489-014-0613-2

Chen, Y. & Hao, Y. (2017). A feature weighted support vector machine and K-nearest neighbor algorithm for stock market indices prediction. *Expert Systems with Applications, 80*, 340-355. doi:10.1016/j.eswa.2017.02.044

Cruz, A., Caldas, L., Mendes, V., Mendes, J. & Bastos, L. (2024). Multi-objective optimization based on surrogate models for sustainable building design: A systematic literature review. *Building and Environment, 266*, 112147. doi:10.1016/j.buildenv.2024.112147

Es-sakali, N., Pfafferott, J., Mghazli, M. O. & Cherkaoui, M. (2025). Towards climate-responsive net zero energy rural schools: A multi-objective passive design optimization with bio-based insulations, shading, and roof vegetation. *Sustainable Cities and Society, 120*, 106142. doi:10.1016/j.scs.2025.106142

Evins, R. (2013). A review of computational optimisation methods applied to sustainable building design. *Renewable and Sustainable Energy Reviews, 22*, 230-245. doi:10.1016/j.rser.2013.02.004

Fang, Y. & Cho, S. (2019). Design optimization of building geometry and fenestration for daylighting and energy performance. *Solar Energy, 191*, 7-18. doi:10.1016/j.solener.2019.08.039

Gupta, V. & Deb, C. (2023). Envelope design for low-energy buildings in the tropics: A review. *Renewable and Sustainable Energy Reviews, 186*, 113650. doi:10.1016/j.rser.2023.113650

Han, Z., Li, X., Sun, J., Wang, M. & Liu, G. (2023). An interactive multi-criteria decision-making method for building performance design. *Energy and Buildings, 282*, 112793. doi:10.1016/j.enbuild.2023.112793

Hansen, N., Müller, S. D. & Koumoutsakos, P. (2003). Reducing the time complexity of the derandomized evolution strategy with covariance matrix adaptation (CMA-ES). *Evolutionary Computation, 11*(1), 1-18. doi:10.1162/106365603321828970

He, Q., Wu, Z. & Chen, X. (2024). An integrated framework for automatic green building evaluation: A case study of China. *Frontiers of Engineering Management, 11*, 269–287. doi:10.1007/s42524-023-0274-0

Hester, J., Gregory, J., Ulm, F.-J. & Kirchain, R. (2018). Building design-space exploration through quasi-optimization of life cycle impacts and costs. *Building and Environment, 144*, 34-44. doi:10.1016/j.buildenv.2018.08.003

Hinkle, L. E., Pavlak, G., Curtis, L. & Brown, N. C. (2024). Implementing dynamic subset sensitivity analysis for early design datasets. *Automation in Construction, 158*, 105198. doi:10.1016/j.autcon.2023.105198

Hinkle, L. E., Wang, J. & Brown, N. C. (2022). Quantifying potential dynamic façade energy savings in early design using constrained optimization. *Building and Environment, 221*, 109265. doi:10.1016/j.buildenv.2022.109265

HKHA. (2015). *Design of the new public housing flats by the Hong Kong Housing Authority.* Transport and Housing Bureau. Hong Kong: Legislative Council Panel on Housing. Retrieved 12 2, 2024, from https://www.legco.gov.hk/yr14-15/english/panels/hg/papers/hg20150706cb1-1037-1-e.pdf

Javanroodi, K., Nik, V. M. & Mahdavinejad, M. (2019). A novel design-based optimization framework for enhancing the energy efficiency of high-rise office buildings in urban areas. *Sustainable Cities and Society, 49*, 101597. doi:10.1016/j.scs.2019.101597

Kämpf, J. H., Wetter, M. & Robinson, D. (2010). A comparison of global optimization algorithms with standard benchmark functions and real-world applications using EnergyPlus. *Journal of Building Performance Simulation, 3*(2), 103-120. doi:10.1080/19401490903494597

Katoch, S., Chauhan, S. S. & Kumar, V. (2021). A review on genetic algorithm: past, present, and future. *Multimedia Tools and Applications, 80*, 8091–8126. doi:10.1007/s11042-020-10139-6

Konis, K., Gamas, A. & Kensek, K. (2016). Passive performance and building form: An optimization framework for early-stage design support. *Solar Energy, 125*, 161-179. doi:10.1016/j.solener.2015.12.020

Kotsiantis, S. B. (2013). Decision trees: a recent overview. *Artificial Intelligence Review, 39*, 261-283. doi:10.1007/s10462-011-9272-4

Li, X., Lu, W., Peng, Z., Zhang, Y. & Huang, J. (2024). Generative design of walkable urban cool spots using a novel heuristic GAN×GAN approach. *Building and Environment, 266*, 112027. doi:10.1016/j.buildenv.2024.112027

Lin, B., Chen, H., Yu, Q., Zhou, X., Lv, S., He, Q. & Li, Z. (2021). MOOSAS – A systematic solution for multiple objective building performance optimization in the early design stage. *Building and Environment, 200*, 107929. doi:10.1016/j.buildenv.2021.107929

Liu, K., Xu, X., Huang, W., Zhang, R., Kong, L. & Wang, X. (2023). A multi-objective optimization framework for designing urban block forms considering daylight, energy consumption, and photovoltaic energy potential. *Building and Environment, 242*, 110585. doi:10.1016/j.buildenv.2023.110585

Liu, R., Liu, Z., Xiong, W., Zhang, L., Zhao, C. & Yin, Y. (2024). Performance simulation and optimization of building façade photovoltaic systems under different urban building layouts. *Energy, 288*, 129708. doi:10.1016/j.energy.2023.129708

Liu, X., Tang, H., Ding, Y. & Yan, D. (2022). Investigating the performance of machine learning models combined with different feature selection methods to estimate the energy consumption of buildings. *Energy and Buildings, 273*, 112408. doi:10.1016/j.enbuild.2022.112408

Luca, F. D., Natanian, J. & Wortmann, T. (2024). Ten questions concerning environmental architectural design exploration. *Building and Environment, 261*, 111697. doi:10.1016/j.buildenv.2024.111697

Machairas, V., Tsangrassoulis, A. & Axarli, K. (2014). Algorithms for optimization of building design: A review. *Renewable and Sustainable Energy Reviews, 31*, 101-112. doi:10.1016/j.rser.2013.11.036

MOHURD. (2018). *Standard for urban residential area planning and design.* MOHURD Research Institute of Standards and Norms, Ministry of Housing and Urban-Rural Development. People's Republic of China: China Architecture & Building Press. Retrieved 1 2, 2025, from https://www.codeofchina.com/standard/GB50180-2018.html

Mousavi, S., Gijón-Rivera, M., Rivera-Solorio, C. & Rangel, C. G. (2022). Energy, comfort, and environmental assessment of passive techniques integrated into low-energy residential buildings in semi-arid climate. *Energy and Buildings, 263*, 112053. doi:10.1016/j.enbuild.2022.112053

Nguyen, A.-T., Reiter, S. & Rigo, P. (2014). A review on simulation-based optimization methods applied to building performance analysis. *Applied Energy, 113*, 1043-1058. doi:10.1016/j.apenergy.2013.08.061

Olu-Ajayi, R., Alaka, H., Sulaimon, I., Sunmola, F. & Ajayi, S. (2022). Building energy consumption prediction for residential buildings using deep learning and other machine learning techniques. *Journal of Building Engineering, 45*, 103406. doi:10.1016/j.jobe.2021.103406

Omuya, E. O., Okeyo, G. O. & Kimwele, M. W. (2021). Feature selection for classification using principal component analysis and information gain. *Expert Systems with Applications, 174*, 114765. doi:10.1016/j.eswa.2021.114765

Østergård, T., Jensen, R. L. & Maagaard, S. E. (2017). Early Building Design: Informed decision-making by exploring multidimensional design space using sensitivity analysis. *Energy and Buildings, 142*, 8-22. doi:10.1016/j.enbuild.2017.02.059

Qin, H. & Pan, W. (2020). Energy use of subtropical high-rise public residential buildings and impacts of energy saving measures. *Journal of Cleaner Production, 254*, 120041. doi:10.1016/j.jclepro.2020.120041

Ramallo-González, A. & Coley, D. (2014). Using self-adaptive optimisation methods to perform sequential optimisation for low-energy building design. *Energy and Buildings, 81*, 18-29. doi:10.1016/j.enbuild.2014.05.037

Rehbach, F., Zaefferer, M., Fischbach, A., Rudolph, G. & Bartz-Beielstein, T. (2022). Benchmark-driven configuration of a parallel model-based optimization algorithm. *IEEE Transactions on Evolutionary Computation, 26*(6), 1365-1379. doi:10.1109/TEVC.2022.3163843

Roudsari, M. S. & Pak, M. (2013). Ladybug: A parametric environmental plugin for grasshopper to help designers create an environmentally-conscious design. *Proceedings of the 13th international IBPSA conference* (pp. 3128-3135). Lyon, France: Building Simulation Conference Proceedings. doi:10.26868/25222708.2013.2499

Shannon, C. E. (1948). A mathematical theory of communication. *The Bell system technical journal, 27*(3), 379 - 423. doi:10.1002/j.1538-7305.1948.tb01338.x

Showkatbakhsh, M. & Makki, M. (2022). Multi-Objective Optimisation of Urban Form: A Framework for Selecting the Optimal Solution. *Buildings, 12*(9), 1473. doi:10.3390/buildings12091473

Son, K. & Hyun, K. H. (2022). Designer-Centric Spatial Design Support. *Automation in Construction, 137*, 104195. doi:10.1016/j.autcon.2022.104195

Son, K., Lee, S. W., Yoon, W. & Hyun, K. H. (2022). CreativeSearch: Proactive design exploration system with Bayesian information gain and information entropy. *Automation in Construction, 142*, 104502. doi:10.1016/j.autcon.2022.104502

Tian, L., Hao, T., He, X., Chan, I., Niu, J., Chan, P., Ng, W. & Huang, J. (2024). Examining the non-linear relationship between urban form and air temperature at street level: A case of Hong Kong. *Building and Environment, 264*, 111884. doi:10.1016/j.buildenv.2024.111884

Tian, W. (2013). A review of sensitivity analysis methods in building energy analysis. *Renewable and Sustainable Energy Reviews, 20*, 411-419. doi:10.1016/j.rser.2012.12.014

UNEP. (2024). *Global status report for buildings and construction: Beyond foundations: Mainstreaming sustainable solutions to cut emissions from the buildings sector.* Nairobi: United Nations Environment Programme. Retrieved 11 28, 2024, from https://www.unep.org/resources/report/global-status-report-buildings-and-construction

Waibel, C., Wortmann, T., Evins, R. & Carmeliet, J. (2019). Building energy optimization: An extensive benchmark of global search algorithms. *Energy and Buildings, 187*, 218-240. doi:10.1016/j.enbuild.2019.01.048

Wang, X., Teigland, R. & Hollberg, A. (2024). Identifying influential architectural design variables for early-stage building sustainability optimization. *Building and Environment, 252*, 111295. doi:10.1016/j.buildenv.2024.111295

Weerasuriya, A., Zhang, X., Wang, J., Lu, B., Tse, K. & Liu, C.-H. (2021). Performance evaluation of population-based metaheuristic algorithms and decision-making for multi-objective optimization of building design. *Building and Environment, 198*, 107855. doi:10.1016/j.buildenv.2021.107855

Wortmann, T. (2019). Genetic evolution vs. function approximation: Benchmarking algorithms for architectural design optimization. *Journal of Computational Design and Engineering, 6*(3), 414-428. doi:10.1016/j.jcde.2018.09.001

Wortmann, T., Cichocka, J. & Waibel, C. (2022). Simulation-based optimization in architecture and building engineering—Results from an international user survey in practice and research. *Energy and Buildings, 259*, 111863. doi:10.1016/j.enbuild.2022.111863

Xue, F., Lu, W., Chen, K. & Zetkulic, A. (2019). From Semantic Segmentation to Semantic Registration: Derivative-Free Optimization–Based Approach for Automatic Generation of Semantically Rich As-Built Building Information Models from 3D Point Clouds. *Journal of Computing in Civil Engineering, 33*(4), 04019024. doi:10.1061/(ASCE)CP.1943-5487.0000839

Yu, S., You, L. & Zhou, S. (2023). A review of optimization modeling and solution methods in renewable energy systems. *Frontiers of Engineering Management, 10*, 640–671. doi:10.1007/s42524-023-0271-3

Zhan, J., He, W. & Huang, J. (2024). Comfort, carbon emissions, and cost of building envelope and photovoltaic arrangement optimization through a two-stage model. *Applied Energy, 356*, 122423. doi:10.1016/j.apenergy.2023.122423

Zhang, Z., Geng, Y., Wu, X., Zhou, H. & Lin, B. (2022). A method for determining the weight of objective indoor environment and subjective response based on information theory. *Building and Environment, 207*, 108426. doi:10.1016/j.buildenv.2021.108426

Zhou, Q. & Xue, F. (2023). Pushing the boundaries of modular-integrated construction: A symmetric skeleton grammar-based multi-objective optimization of passive design for energy savings and daylight autonomy. *Energy and Buildings, 296*, 113417. doi:10.1016/j.enbuild.2023.113417

Zhou, Y., Ma, M., Tam, V. W. & Le, K. N. (2023). Design variables affecting the environmental impacts of buildings: A critical review. *Journal of Cleaner Production, 387*, 135921. doi:10.1016/j.jclepro.2023.135921

Appendix A. Supplementary table and figures of experiments

This section shows the detailed settings in experiments.

Table A.1. Baseline settings for the original one-bedroom modular flat (Case 1).
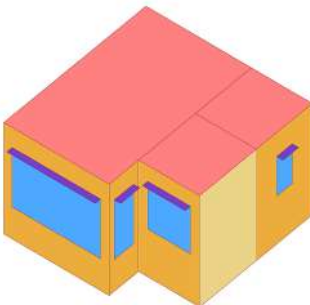
Category	Items	Values	Unit	Baseline model
Simulation setting	Location	Hong Kong SAR	-	EUI = 159.599 kWh/m^2·yr
	Climate zone	2-Hot	-	
	Construction set	ASHRAE 90.1 2019	-	
	HVAC system	Window AC with no heat	-	
	Grid size (G_{s1})	0.2	m	
Window parameters setting	WWR_1	0.45	-	
	WWR_2	0.35	-	
	WWR_3	0.30	-	
	WWR_4	0.10	-	
	$WH_{1\&2}$	1.5	m	
	WH_3	1.2	m	
	WH_4	1	m	
	$WSH_{1\&2}$	0.80	m	
	WSH_3; WSH_4	1.20	m	
Window louver parameters setting	LC_1; LC_2; LC_3; LC_4	1	-	
	LA_1; LA_2; LA_3; LA_4	0	°	
	LVH_1; LVH_2; LVH_3; LVH_4	0	-	

Table A.2. Baseline settings for the urban block forms optimization (Case 2).
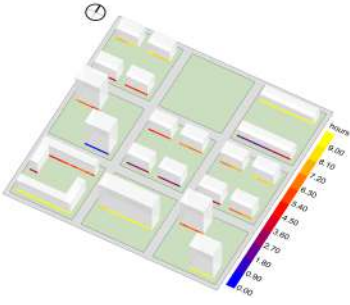
Category	Items	Values	Unit	Baseline model
Simulation setting	Location	Jianhu City, Jiangsu Province	-	DSH = 6.081 hours
	Grid size (G_{s2})	1	m	
	Date and time	Jan. 20th 8:00-16:00	-	
Building types position	$OPos$	5	-	
	Pos_1	C-2	-	
	Pos_2	P-4	-	
	Pos_3	P-2	-	
	Pos_4	S-3	-	
	Pos_5	P-2	-	
	Pos_6	P-4	-	
	Pos_7	P-2	-	
	Pos_8	S-2	-	
Window louver parameters setting	NF_{P1}	2	-	
	NF_{S1}	1	-	
	NF_{C1}	3	-	
	NF_{P2}	6	-	
	NF_{S2}	4	-	
	NF_{C2}	6	-	
	NF_{P3}	30	-	
	NF_{P4}; NF_{S3}	13	-	

Table A.3. Hyperparameters settings for single-objective algorithms.

Algorithm	Grasshopper plugin	Hyperparameters	Description	Value
GA	Galapagos	Population size	Number of individuals in each generation	25
		Initial boost	Controlling the exploration range in the first generation	2
		Max. Stagnant	Managing convergence efficiency	50
		Elite rate	Preserving best individuals across generations	5%
		Inbreeding rate	Controlling genetic diversity by probability of parent solutions' exchange	75%
CMA-ES	Opossum	Initial sigma	Controls the initial step size of the search range	0.5
RBFOpt	Opossum	Max. iterations	The maximum number of iterations	10000
		Max. evaluations	The maximum number of evaluations	10000
		Max. stalled cycles	The maximum number of consecutive iterations allowed without significant improvement in the objective function value	2000
		Local search box scaling	Limit the scope of the local search	False